Available online at www.sciencedirect.com
SCIENCE DIRECT®
Catalysis Today 105 (2005) 629–633
CATALYSIS TODAY
www.elsevier.com/locate/cattod

Role of Al segregation and high affinity to oxygen in formation of adhesive alumina layers on FeCr alloy support

J. Camra [a], E. Bielańska [b], A. Bernasik [c], K. Kowalski [d], M. Zimowska [e], A. Białas [e], M. Najbar [e,*]

[a] *Regional Laboratory of Physicochemical Analyses and Structural Research, 30 060 Kraków, Ingardena 3, Poland*
[b] *Institute of Metallurgy and Material Science, Polish Academy of Sciences, 30 059 Kraków, Reymonta 25, Poland*
[c] *Faculty of Physics and Applied Computer Science, AGH – University of Science and Technology, Mickiewicza 30, 30-059 Kraków, Poland*
[d] *Faculty of Metallurgy and Materials Science, AGH – University of Science and Technology, Mickiewicza 30, 30-059 Kraków, Poland*
[e] *Department of Chemistry, Jagiellonian University, 30 060 Kraków, Ingardena 3, Poland*

Abstract

The aim of this study is to gain information necessary to propose the mechanism of the oxide layers' formation on the FeCr alloy foil of 0.05 mm thickness as well as to obtain indications about thermal treatment resulting in the relatively uniform adhesive layers.

The surface morphology of the oxide layers formed on the foil in the course of its thermal treatment as well as layers' thickness and element distribution along their cross sections were investigated with scanning electron microscopy and secondary ion mass spectrometry. Observed differences were ascribed to the various orientations of FeCr alloy crystallites.

Keywords: 0.05 mm FeCr alloy foil; Y and Al surface segregation; Y and Al high affinity to oxygen; Outward Al cation diffusion

1. Introduction

The growing attention has recently been paid to metallic monoliths due to good thermal conductivity and plasticity of metals [1,2]. Many different metals and alloys were investigated as promising materials for metallic monoliths production. Kanthal and FeCr alloy were revealed to be the most suitable ones. The crucial point in the production of the monolithic catalysts on metallic supports is the formation of stable porous layers on the metallic foil surface. According to US patents [3,4] annealing FeCr alloy foil at 1273 K in oxygen containing atmosphere causes formation of the whisker crystallites on its surface. The authors of the patents did not give information about chemical and phase composition of those crystallites. According to our patent [5], programmed heating of the FeCr alloy foil of 0.1 mm thickness in air from room temperature to 1113 K results in the formation of the quite uniform adhesive alumina layer of ca. 2 μm thickness, with some Fe and Cr ions incorporated into its structure. This layer exposes the scale-like crystallites, very suitable to be filled by alumina washcoat. As formed layer was found to contain mainly α-alumina [6]. The growing demands concerning the thickness of the channels' walls cause growing interest in the formation of the adhesive layers on the surface of the FeCr alloy foil of smaller thickness.

Back scattered electron images of the fresh FeCr alloy foil of 0.05 mm thickness [7] revealed that the foil surface is composed of regular areas of diameter of several μm showing different ability to scatter electrons. It suggested that it is composed of different faces of FeCr alloy crystallites probably covered by the thin oxide layer of different thickness.

The aim of this paper was: investigation of the thickness and chemical composition of the oxide layers on the fresh 0.05 mm foil as well as on the one thermally treated,

* Corresponding author. Tel.: +48 12 63 36 377; fax: +48 12 63 40 515.
E-mail address: mnajbar@chemia.uj.edu.pl (M. Najbar).

0920-5861/$ – see front matter © 2005 Elsevier B.V. All rights reserved.
doi:10.1016/j.cattod.2005.06.015

according to the procedure previously used for scale crystallite formation on 0.1 mm foil [7].

It was thought that the results would allow to understand the reason of the differences in the surface morphology of both the foils and to propose thermal treatment procedure resulting in the formation of the relatively uniform adhesive alumina layers on 0.05 mm foil.

2. Experimental

The FeCr alloy foil used in the experiments consists of ca. 74 wt.% Fe, 20 wt. % Cr, 5 wt.% Al and less than 1 wt.% Y. It was supplied by A.S. THEIS Stahltechnologie Hagen-Holden, Germany. The foil samples after washing in acetone were heated at 3 K min^{-1} to 873 K and then again at 0.5 K min^{-1} to 1113 K in air. They were next chilled to room temperature in air with the average rate 2 K min^{-1}.

The morphology of the foil surface and the chemical composition in the surface microlayers were investigated with a Philips Scanning Electron Microscope (SEM) XL with an EDS LINK-ISIS system.

The thickness of the thickest oxide layers and their chemical composition as a depth function were determined with secondary ion mass spectrometry (SIMS). Gallium gun with field emission, FEI Company and a Balzers guadrupole spectrometer – a part of a VSW XPS-SIMS spectrometer, were used. Sputtering factors were calculated with SRIM 2000 program.

3. Results and discussion

Fig. 1 presents back scattered electron (BSE) (A) and secondary electron SE (B) images (1000×) of the chosen area of the foil subject to above described thermal treatment.

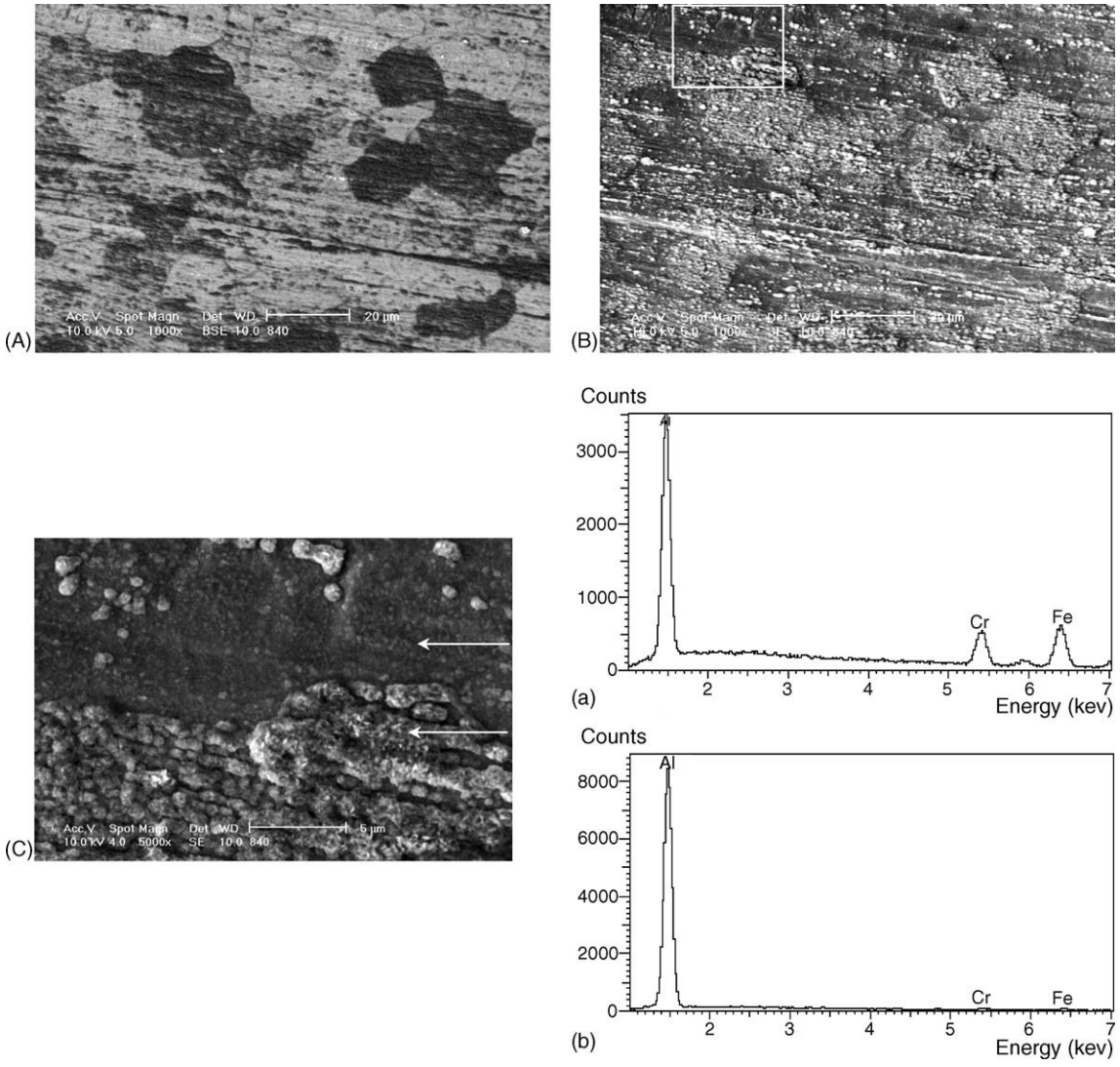

Fig. 1. SEM characterisation of the FeCr alloy foil heated at 3 K min^{-1} to 873 K and then at 0.5 K min^{-1} to 1113 K in air and next annealed at this temperature in air for 13 h: (A) back scattered electron (BSE) image (1000×), (B) secondary electron (SE) image (1000×), (C) SE image (5000×) of the area marked in (B), (a) and (b) energy dispersive spectra (EDS) from the microareas pointed in (C).

The brighter areas in BSE image correspond to the darker areas in SE one. It means that areas better scattering the electrons do not easily emit the secondary electrons and vice versa the areas weaker scattering the electron bean better emit the secondary electrons. To reveal the reason of the observed differences of contrasts in BSE and SE images the enlarged SE image (5000×) of the area marked in Fig. 1B is shown in C. As seen the brighter area is rough and built from the separate islands composed of needle-like crystallites with the width of several tens nanometres. Whereas the darker area looks like the continuous layer with growing up hardly seen small crystallites. The energy dispersion spectrum taken from the rough area contains practically only aluminium peak. Whereas the distinct peaks of iron and chromium are present in the spectrum taken from the darker area. Therefore it can be thought that the alumina layer is larger or equal to the depth of emission of the characteristic X-radiation in the rough area, and it is smaller in the continuous area. According to Pietruszka et al. [6], the oxide layer formed on FeCr alloy foil of the 0.1 mm thickness contains mainly α-alumina. The depth of the characteristic X-ray radiation emission (10 keV) from α-alumina (calculated with the use of the Anderson-Hasler equation [8]) is equal to 0.75 μm. Thus, the thickness of the oxide layer in the rough area is equal to or bigger than 0.75 μm and the thickness in the continuous areas is smaller than 0.75 μm. One can say that the lighter areas in BSE image contain more heavier Cr and Fe atoms than lighter ones. Whereas the lighter areas in SE image contain more small needle-like crystallites of high secondary electrons' emission than darker ones. It can be thus thought that the surface of the 0.05 mm foil is built of the alloy crystallites' faces on which aluminium segregation followed by alumina formation occur with the different rates.

In Fig. 2A and B SIM analyses of the fresh foil, as cations' and anions' intensities against the distances from the foil surfaces (ca. 10^4 μm^2, sputtering rate equal to ca. 15 nm min^{-1}) are presented. As the ions' sputtering from the oxide phase is much easier than from the alloy their signals are the highest closely to the surface and decreases as the contribution of the metallic phase increases. Because of the very low concentration of CrO^-, FeO^- and YO^- ions their depth profiles are illegible. The presence of Cr and Fe ions in the top oxide layers (Fig. 2A) shows that iron and chromium also take part in the oxide formation.

The shapes of the depth profiles confirm SEM observations [7] that the foil surface is not totally smooth but it contains thinner or thicker parts of the oxide phase.

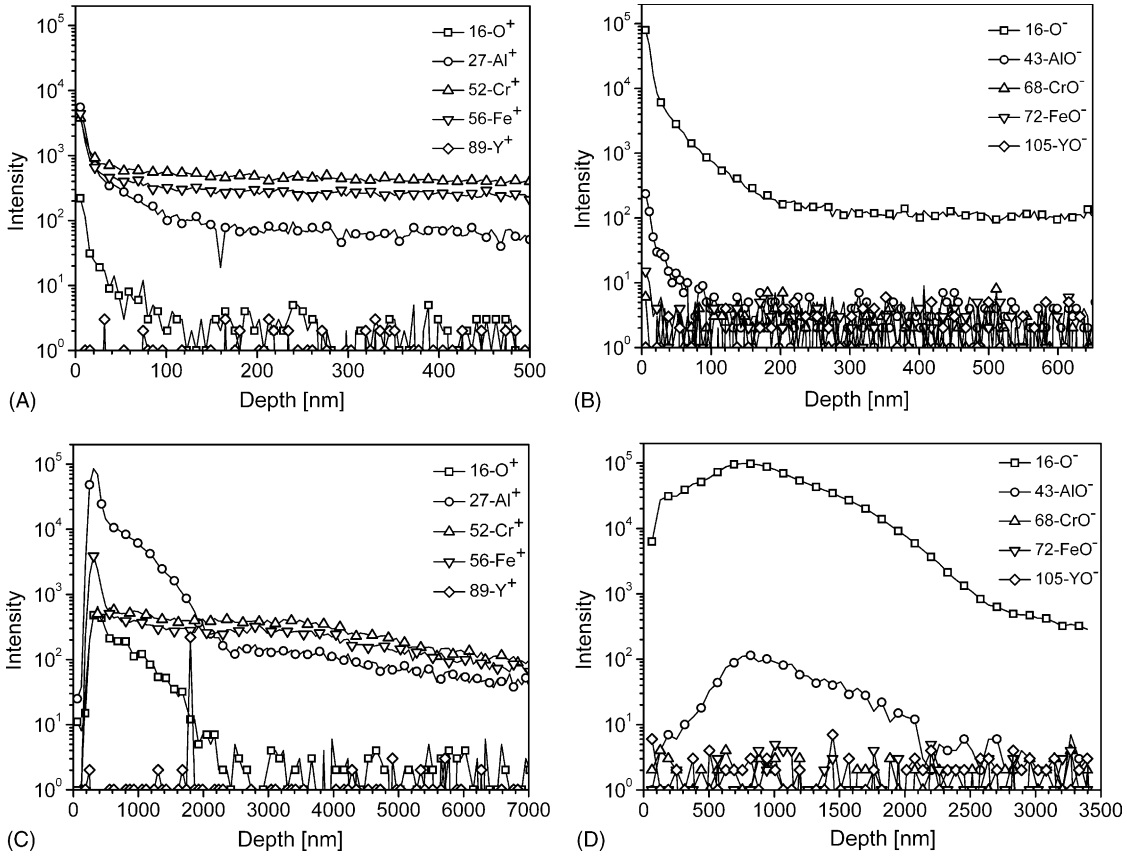

Fig. 2. SIMS characterisation of the FeCr alloy foil: (A) the O^+, Al^+, Cr^+, Fe^+, Y^+ depth profiles for the fresh foil, (B) the O^-, AlO^-, CrO^-, FeO^-, YO^- depth profiles for the fresh foil, (C) the O^+, Al^+, Cr^+, Fe^+, Y^+ depth profiles for the foil heated at 3 K min^{-1} to 873 K and then at 0.5 K min^{-1} to 1113 K in air and next annealed at this temperature also in air for 13 h, (D) the O^-, AlO^-, CrO^-, FeO^-, YO^- depth profiles for the foil heated at 3 K min^{-1} to 873 K and then at 0.5 K min^{-1} to 1113 K in air and next annealed at this temperature also in air.

The thickness of the thickest alumina layer estimated from Fe^+ and Cr^+ depth profiles is equal to 80 nm and a plateaux on Al^+ depth profile as well as distinct lowering of the slope of O^- depth profile begin at 170 nm. The observed shift of the enhanced aluminium and oxygen concentrations toward deeper layers can be ascribed to the thin alumina layers formed between the FeCr alloy crystallites. A sharp minimum on Al^+ depth profile at 170 nm may be connected with the surface aluminium segregation. The small decrease in the O^- concentration below 170 nm can be ascribed to the decreasing amount of oxygen dissolved in FeCr alloy structure.

Fig. 2C and D present the cation and anion depth profiles (sputtering rate equal to ca 75 nm min^{-1}) for the thermally treated foil. The initial increase of the amounts of the sputtered ions with the depth can be ascribed to the surface morphology (Fig. 1C). As can be noticed, the thickness of the thickest oxide layer estimated from Fe^+ and Cr^+depth profiles is equal to ca. 1800 nm. A plateaux on the Al^+ depth profile and a distinct lowering of the slope of O^- depth profile, coming from inter-crystallite alumina, begin at almost the same depth, 2500 and 2800 ppm, respectively (the small difference may be connected with some differences in the surface morphology as the analyses were done separately). Similarly as in the case of the fresh foil iron is present in the top oxide layers (Fig. 2C) what confirms its participation in oxide layers' growth. However, the shallow local minimum on the Cr depth profile at ca 470 nm (Fig. 2C) reveals sublimation of CrO_3 formed due to surface chromium segregation. Such a depth profile was earlier observed in V–O–Mo system in which surface molybdena undergoes sublimation [9]. The sharp maximum on a yttrium depth profile at oxide/alloy boundary distinctly shows that Y segregates on the FeCr alloy crystallite surface but does not diffuse into alumina layer.

4. Discussion

It is worthy to note that the maximum of yttrium concentration occurs in the distance of 1.8 μm from the top of the oxide layer thus in the bottom of the thickest oxide layer. It means that yttrium segregates preferably on the same surfaces of the alloy grains on which aluminium segregates the most intensively. It can be expected that, the large yttrium (r = 182 pm [10]) and aluminium (r = 143 pm [10]) atoms diffuse preferentially to crystallite surfaces cross the planes with the loosest packed atoms and do not participate in the oxide layer formation. The strains caused in the alloy structure by the presence of atoms much larger than basal Fe ones (r = 126 pm [10]) should be a driving force of that diffusion. The affinity to oxygen of yttrium (ΔH_f^θ (Y_2O_3) = 1905.3 kJ/mol) is higher than of aluminium (ΔH_f^θ (Al_2O_3) = 1675.7 kJ/mol), much higher than of chromium (ΔH_f^θ (Cr_2O_3) = 1139.7 kJ/mol) and very much higher than of iron (ΔH_f^θ (Fe_2O_3) = 824.2 kJ/mol [11]). It can be thus thought that yttrium is incorporated in the bottom oxide layer and due to its high m/q ratio and relatively big radius stays in this layer. Thus oxide layers are formed mostly due to aluminium cations' diffusion. They are formed due to high aluminium affinity to oxygen and their diffusion is facilitated by low m/q ratio and relatively small radius. Diffusion of the iron and chromium ions are limited for the same reason.

To obtain the uniform layer, the oxidation should be performed at higher temperatures resulting in lowering the dependence of Al diffusion rate on the direction.

In the light of the above discussion, one can think that the scale-like crystallites grown on 0.1 mm foil [5–6] are anchored between FeCr alloy crystallites exposing close packed surfaces.

The mutual orientation of the FeCr alloy crystalites and alumina epitaxial layers will be the subject of the next publication [12].

5. Conclusions

The surface morphology, thickness and particular elements' depth profiles for the oxide layers formed on 0.05 mm FeCr alloy foil, heated to 1113 K and annealed at this temperature, were investigated.

The study gave information necessary to propose a mechanism of the oxide adhesive layer formation.

The aluminum and yttrium segregation was revealed to be the first step of the oxide formation. The surface Al cation diffusion was shown to be mostly responsible for the oxide layer growth. Y cations were found to be immobile, staying in the bottom of the oxide layer.

The surface of the foil is structured of the different FeCr alloy faces. The alumina layers with different thickness and morphology grow on crystallites of different orientations.

The way of foil thermal treatment leading to relatively uniform adhesive layer formation is proposed.

Acknowledgement

One of us (A. Bernasik) expresses his gratitude to Polish State Committee for Scientific Research for financial support.

References

[1] S. Irandoust, B. Andersson, Catal. Rev. Sci. Eng. 30 (3) (1988) 341.
[2] A. Cybulski, J.A. Moulijn, Rev. Sci. Eng. 36 (2) (1994) 179.
[3] L. Chapman, US patent 4 318 828, 1982.
[4] L. Chapman, C. Vigor, J. Watton, US patent 4 331, 631, 1982.
[5] M. Najbar, A. Steiner, A. Białas, E. Bielańska, J. Camra, P 183 (2002) 563.
[6] B. Pietruszka, M. Najbar, L. Lityńska-Dobrzyńska, E. Bielańska, M. Zimowska, J. Camra, Stud. Surf. Sci. Catal. 136 (2001) 471.

[7] M. Najbar, J. Camra, M. Zimowska, A. Białas, E. Bielańska, Pol. J. Env. Stud. 11 (2002) 35, Suppl. III.
[8] C. Anderson, M. Hasler, X-ray Optics and Microanalysis, Herman, Paris, 1966 , p. 310.
[9] M. Najbar, Proc. 8th Int. Congress on Catal., Berlin 5, 1984, p. 323.
[10] D.F. Shriver, P.W. Atkins, C.H. Langford, Inorganic Chemistry, Oxford University Press, Oxford, Melbourne, Tokyo, 1990 , p. 26.
[11] CRC Handbook of Chemistry and Physics, 85th ed., CRC Press, Boca Raton, London, New York, Washington D.C., 2004, pp. 5–6, 5–13, 5–16, 5–23.
[12] B. Borzęcka Prokop, M. Najbar, A. Białas, (in preparation).